

## Multidimensional Coherent Spectroscopy of Molecular Polaritons: Langevin Approach

Zhedong Zhang<sup>1,2,\*</sup>, Xiaoyu Nie<sup>3</sup>, Danyuan Lei<sup>4</sup>, and Shaul Mukamel<sup>5,†</sup>

<sup>1</sup>Department of Physics, City University of Hong Kong, Kowloon, Hong Kong SAR

<sup>2</sup>City University of Hong Kong, Shenzhen Research Institute, Shenzhen, Guangdong 518057, China

<sup>3</sup>School of Physics, Xi'an Jiaotong University, Xi'an, Shaanxi 710049, China

<sup>4</sup>Department of Materials Science and Engineering, City University of Hong Kong, Kowloon, Hong Kong SAR

<sup>5</sup>Department of Chemistry, Department of Physics and Astronomy, University of California Irvine, Irvine, California 92697, USA



(Received 8 August 2022; accepted 3 January 2023; published 10 March 2023)

We present a microscopic theory for nonlinear optical spectroscopy of  $N$  molecules in an optical cavity. Using the Heisenberg-Langevin equation, an analytical expression is derived for the time- and frequency-resolved signals accounting for arbitrary numbers of vibrational excitations. We identify clear signatures of the polariton-polaron interaction from multidimensional projections of the signal, e.g., pathways and timescales. Cooperative dynamics of cavity polaritons against intramolecular vibrations is revealed, along with a crosstalk between long-range coherence and vibronic coupling that may lead to localization effects. Our results further characterize the polaritonic coherence and the population transfer that is slower.

DOI: [10.1103/PhysRevLett.130.103001](https://doi.org/10.1103/PhysRevLett.130.103001)

**Introduction.**—Strong molecule-photon interaction has drawn considerable attention in recent study of molecular spectroscopy. New relaxation channels have been demonstrated to control fast electron dynamics and reaction activity [1–9]. Optical cavities create hybrid states between molecules and confined photons, known as polaritons [10–13]. Theoretically, this requires a substantial generalization of quantum electrodynamics (QED) into molecules containing many more degrees of freedom than atoms and qubits.

It has been demonstrated that light in a confined geometry can significantly alter the molecular absorption and emission signals [14–17]. The collective interaction between many molecules and photons is of fundamental importance, leading to interesting phenomena, e.g., superradiance and cooperative dynamics of polaritons [18–22]. In contrast to atoms, whereby superradiance and cavity polaritons are well understood, molecular polaritons are more complex. This arises from the complicated couplings between electronic and nuclear degrees of freedom, which possess new challenges for optical spectroscopy. Recently, exact diagonalization of molecular Hamiltonian was used to calculate the optical responses, by taking only a few vibrational excitations into account [11,23–25]. Here, we focus on the polaritonic relaxation pathways involving the population and coherence dynamics, which are, however, open issues. A quantum dynamics of molecular polaritons using wave packets was developed, manifesting the relaxation between polaritons and dark states [26]. Collective nonadiabatic transitions were, thus, predicted from a connection between the Tavis-Cummings and Jahn-Teller Hamiltonians. An ultrafast spectroscopic technique has been used to monitor the dynamics of vibrational polaritons

[21,27]. Time- and frequency-gated photon-coincidence counting was employed to monitor the many-body dynamics of cavity polaritons, making use of nonlinear interferometry [28,29]. Polaritons reveal the effects of strongly modifying the energy harvesting and migration in chromophore aggregates, through novel control knobs not accessible by classical light [7,8,13,30–32]. Elaborate nonlinear optical measurements of molecular polaritons have demonstrated unusual correlation properties [33–35]. That calls for an extensive understanding of dark states with a high mode density [36–40], nonlinearities, and multiexciton correlations [41–44].

Previous spectroscopic studies of cavity polaritons were mostly based on wave function methods involving nuclear dynamics [45–48], Redfield theory, and quantum chemistry simulations of low excitations [49–53]. Absorption and emission associated with multiple phonons and optically dark states depend on a strong polariton-polaron interaction, which raises a fundamental issue in cavity polaritons and, however, complicates the simulation of ultrafast spectroscopy.

In this Letter, we develop a quantum Langevin theory for time-frequency-resolved coherent spectroscopy of molecular polaritons. We adopt the two-level description for molecules coupled to intramolecular vibrations undergoing the Brownian oscillation. This is along with the Holstein-Tavis-Cummings model. Subject to sequential laser pulses, an analytical solution for multidimensional third-order spectroscopic signals is developed. The results reveal multiple channels and timescales of the cooperative relaxation of polaritons and also the trade-off with dark states.

**Langevin model for polaritons.**—Given  $N$  identical molecules in an optical cavity, each has two energy surfaces

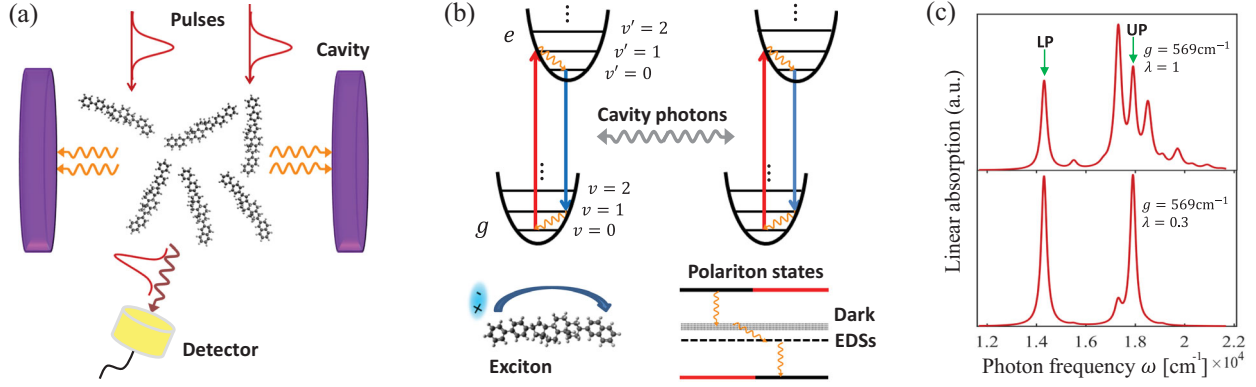


FIG. 1. Schematic of time-resolved spectroscopy for molecular polaritons. (a) Emission signal is collected along a certain direction, once the molecules are excited by laser pulses. (b) Exciton-photon interaction in molecules in the presence of vibronic coupling attached to an individual molecule. This results in the dark states and emitter dark states (EDSs) weakly interacting with the cavity, apart from the upper and lower polariton modes; rich timescales and channels of excited-state relaxation are, thus, expected. (c) Linear absorption of molecular polaritons with ten organic molecules in an optical cavity. The parameters are taken to be  $\omega_D = 16113 \text{ cm}^{-1}$ ,  $\delta = \delta_c = 0$ ,  $\Gamma = 20 \text{ cm}^{-1}$ ,  $\gamma = 1 \text{ cm}^{-1}$ ,  $\gamma_c = 0.9 \text{ cm}^{-1}$ , and  $\omega_v = 1200 \text{ cm}^{-1}$ , typically from cyanine dyes [56].

corresponding to electronically ground and excited states, i.e.,  $|g_j\rangle$  and  $|e_j\rangle$  ( $j = 1, 2, \dots, N$ ), respectively. Electronic excitations forming excitons couple to intramolecular vibrations and to cavity photons, as depicted in Fig. 1(b), and are described by the Holstein-Tavis-Cummings Hamiltonian

$$H = \sum_{n=1}^N [\Delta_n \sigma_n^+ \sigma_n^- + \omega_v b_n^\dagger b_n + g(\sigma_n^+ a + \sigma_n^- a^\dagger)] + \delta_c a^\dagger a, \quad (1)$$

where  $\Delta_n = \delta - \lambda \omega_v (b_n + b_n^\dagger)$  and  $\delta$  denotes the detuning between excitons and the external pulse field.  $[\sigma_n^-, \sigma_m^+] = \sigma_n^- \delta_{nm}$ .  $\sigma_n^+ = |e_n\rangle\langle g_n|$  and  $\sigma_n^- = |g_n\rangle\langle e_n|$  are the respective raising and lowering operators for the excitons in the  $n$ th molecule.  $b_n$  denotes the bosonic annihilation operator of the vibrational mode with a high frequency  $\omega_v$ , in the  $n$ th molecule.  $a$  annihilates cavity photons. Each molecule has one high-frequency vibrational mode. In addition to the strong coupling to the single-longitudinal cavity mode, the molecules are subject to three temporally separated laser pulses with electric fields  $E_j(t - T_j)e^{-i\nu_j(t - T_j)}$ ;  $j = 1, 2, 3$  described by  $V(t) = \sum_{j=1}^3 \sum_{n=1}^N V_{j,n}(t) + \text{H.c.}$  and  $V_{j,n}(t) = -\sigma_n^+ \Omega_j(t - T_j)e^{-i(\nu_j - \nu_3)t} e^{i\nu_j T_j}$ .  $\Omega_j(t - T_j) = \mu_{eg} E_j(t - T_j)$  is the Rabi frequency with the  $j$ th pulse field, and  $\mu_{eg}$  is the molecular dipole moment [54]. The full Hamiltonian is  $H(t) = H + V(t)$ , which yields the quantum Langevin equations (QLEs) for  $\sigma_n^-$ ,  $a$ , and  $b_n$ .

We incorporate the polaron transform via the displacement operator  $D_n = e^{-\lambda(b_n - b_n^\dagger)}$  into the QLE for the dressed operator  $\tilde{\sigma}_n^- = \sigma_n^- D_n^\dagger$ . This is to involve the vibronic coupling to all orders, as it is normally moderate or strong. The QLEs for operators read a matrix form

$$\dot{V} = -\hat{M}V + V^{\text{in}}(t) - i \sum_{j=1}^3 \Omega_j(t - T_j) e^{i\nu_j T_j} e^{-i(\nu_j - \nu_3)t} W_x \quad (2)$$

after a lengthy algebra [57]. The vectors  $V = [\tilde{\sigma}_1^-, \tilde{\sigma}_2^-, \dots, \tilde{\sigma}_N^-, a]^T$  and  $W_x = [(2n_1 - 1)D_1^\dagger, \dots, (2n_N - 1)D_N^\dagger, 0]^T$ ,  $n_l = \tilde{\sigma}_l^+ \tilde{\sigma}_l^-$ .  $V^{\text{in}}(t) = [\sqrt{2\gamma} \tilde{\sigma}_1^{\text{in}}(t), \dots, \sqrt{2\gamma} \tilde{\sigma}_N^{\text{in}}(t), \sqrt{2\gamma_c} a^{\text{in}}(t)]^T$  groups the noise operators originated from exciton decay and cavity leakage. The matrix  $\hat{M}$  in Eq. (2) reads

$$\hat{M} = \begin{pmatrix} i\tilde{\delta} + \gamma & 0 & \cdots & 0 & ig\sigma_1^z D_1^\dagger \\ 0 & i\tilde{\delta} + \gamma & \cdots & 0 & ig\sigma_2^z D_2^\dagger \\ \vdots & \vdots & & \vdots & \vdots \\ 0 & 0 & \cdots & i\tilde{\delta} + \gamma & ig\sigma_N^z D_N^\dagger \\ igD_1 & igD_2 & \cdots & igD_N & i\delta_c + \gamma_c \end{pmatrix}. \quad (3)$$

We solve for the vibration dynamics:  $b_n(t) \approx e^{-i(\omega_v + \Gamma)t} b_n(0) + \sqrt{2\Gamma} \int_0^t e^{-i(\omega_v + \Gamma)(t-t')} b_n^{\text{in}}(t') dt'$ , neglecting the back influence from excitons [53]. Equation (2) represents the dynamics of molecular polaritons. Perturbation theory of the molecule-field interaction  $V(t)$  will be used, and we will calculate two-dimensional signals of photon emission off the cavity axis, as shown in Fig. 1(a). These signals are governed by multipoint Green's functions of dipole operators, which are determined by the exact solution to the QLEs in Eq. (2).

*The polariton emission.*—We first present a general result for the emission spectrum of cavity polaritons. Subject to a probe pulse, Eq. (2) solves for the far-field dipolar radiation governed by the macroscopic polarization

of molecules  $P(t) = \mu_{eg}^* \sum_{i=1}^N \langle \sigma_{i,1}^-(t) \rangle$ . We find the emission signal

$$P_E(\omega, T) = 2i |\mu_{eg}|^2 \sum_{i=1}^N \sum_{l=1}^N \iint_{-\infty}^{\infty} dt d\tau e^{i\omega t} E(\tau - T) \times \theta(t - \tau) e^{-iv(\tau - T)} \langle G_{il}(t - \tau) n_l(\tau) D_l^\dagger(\tau) D_i(t) \rangle, \quad (4)$$

where  $G(t) = \mathcal{T} e^{-\int_0^t \hat{M} dt'}$  is the free propagator. We note that, from the dressed populations  $n_l(\tau) D_l^\dagger(\tau)$ , the cavity polaritons of molecules undergo a dynamics against the local fluctuations from the polaron effect. The polaron-induced localization as a result of dark states will compete with the polariton cooperativity. These can be visualized from the emission signal, which is a real-time monitoring of polariton dynamics through pulse shaping and grating. More advanced information will be elaborated by the multidimensional projections of the signals.

*Linear absorption.*—Assuming  $\omega_v \gg T_b$  that applies for organic molecules at room temperature, the vibrational correlation functions can be evaluated with a vacuum state. Using Eq. (2), the absorption spectra reads  $S_A(\omega) = \sum_{i,l=1}^N \sum_{m=0}^{\infty} S_m^\lambda \delta_{il}^m \text{Re}[\mathcal{G}_{il}(\omega - \xi_m^*)]$ , and  $S_m^\lambda = e^{-\lambda^2} \lambda^{2m} / m!$  is the Franck-Condon factor [58].  $\xi_m = m(\omega_v + i\Gamma)$ , and  $\mathcal{G}_{mn}(\Omega) = \int_0^\infty G_{mn}(t) e^{i\Omega t} dt$  is the Fourier component of  $G(t)$ .  $S_A(\omega)$  resolves the lower polariton (LP) and upper polariton (UP) at  $\omega_{\text{LP/UP}}$ , EDSs at  $\omega_D + m\omega_v$  decoupled from cavity photons. The dark states at  $\omega_D$  are not visible. To see these closely, we assume  $\gamma = \gamma_c$  and  $\tilde{\delta} = \delta_c = 0$ . The peak intensities can be found:

$$\frac{S_A(\omega_D + m\omega_v)}{S_A(\omega_{\text{LP/UP}})} \approx \frac{\lambda^{2m} 2\gamma}{m! m\Gamma}, \quad \frac{S_A(\omega_{\text{LP/UP}} + m\omega_v)}{S_A(\omega_{\text{LP/UP}})} \approx 0 \quad (5)$$

for  $N \gg 1$ . The EDSs may be of comparable intensities with polariton modes. Such spectral-line properties will be shown to be generally true in the time-resolved spectroscopic signals.

Figure 1(c) (top) illustrates the absorption spectra. The LP and UP are prominent from the peaks at 14 300 and 17 900  $\text{cm}^{-1}$  separated by  $2g\sqrt{N}$ . In between, we can observe an extra peak at  $\omega_D + \omega_v$  supporting an EDS decoupled from cavity photons and the large oscillator strength owing to the density of states  $\sim N$ . Figure 1(c) (bottom) shows that the EDSs are masked by the Rabi splitting for weaker vibronic coupling. This, as a benchmark to the strong-coupling case, elaborates the effect of vibronic coupling against the collective coupling to cavity photons. The localized nature of the EDSs is, thus, indicated from eroding the cooperativity between molecules. This will be elaborated in time-resolved spectroscopy.

*2D polariton spectroscopy.*—To have multidimensional projections of emission signal, sequential laser pulses have to interact with the molecular polaritons. The first two pulses populate the excited states, yielding  $n_{l,2}(t) = \sigma_{l,1}^\dagger(t) \sigma_{l,1}^-(t)$ , where the first-order correction  $\sigma_{l,1}^\pm$  is calculated from Eq. (2). We find

$$n_{l,2}(t) D_l^\dagger(t) = \sum_{j=1}^N \sum_{j'=1}^N \iint_0^t dt'' dt' \mathcal{E}_1^*(t' - T_1) \mathcal{E}_2(t'' - T_2) \times G_{lj'}^*(t - t') G_{lj}(t - t'') D_{j'}(t') D_j^\dagger(t'') D_l^\dagger(t). \quad (6)$$

The third-order correction to the polarization follows Eq. (4) when the third pulse serves as a probe. Inserting Eq. (6) into Eq. (4) and considering time-ordered pulses, we therefore proceed to the far-field dipolar radiation along the direction  $\mathbf{k}_s = -\mathbf{k}_1 + \mathbf{k}_2 + \mathbf{k}_3$ , i.e.,  $P(t) = \mu_{eg}^* \sum_{i=1}^N \langle \sigma_{i,3}^-(t) \rangle$ . It gives

$$P(\omega) = 2i \sum_{i,l=1}^N \sum_{j,j'=1}^N \iiint_0^\infty dt d\tau dt'' dt' e^{i\omega t} \mathcal{E}_3(\tau - T_3) \times \mathcal{E}_2(t'' - T_2) \mathcal{E}_1^*(t' - T_1) \langle 0 | G_{il}(t - \tau) G_{lj'}^*(\tau - t') \times G_{lj}(t - t'') D_{j'}(t') D_j^\dagger(t'') D_l^\dagger(\tau) D_i(t) | 0 \rangle, \quad (7)$$

where the four-point correlation function of vibrations  $\langle 0 | D_{j'}(t') D_j^\dagger(t'') D_l^\dagger(\tau) D_i(t) | 0 \rangle$  has to be evaluated explicitly. The 2D signal is usually detected via a reference laser beam (local oscillator field) interfering with the emission. This leads to the heterodyne-detected signal  $S_{2D}(\Omega_3, T, \Omega_1) = \text{Im} \int_0^\infty E_{\text{LO}}^*(\Omega_3) P(\Omega_3) e^{i\Omega_1 \tau} d\tau$ , where  $\tau = T_2 - T_1$  and  $E_{\text{LO}}(\Omega_3)$  is the Fourier component of the local oscillator field. In general, calculating the signal with Eq. (7) is hard due to the integrals over pulse shapes. The procedures can be simplified by invoking the *impulsive approximation* such that the pulse is shorter than the dephasing and solvent timescales [55]. This works for many systems of condensed-phase molecules whose dephasing time is typically  $\sim 100$  fs longer than the laser pulses. The solvent relaxation usually takes place within more than a few picoseconds, noting from the reorganization energy  $\lesssim 30 \text{ cm}^{-1}$  [59,60]. In the optical regime, the ultrafast molecular spectroscopy normally acquires the laser pulses with a duration of  $\sim 6\text{--}30$  fs. We further consider the few-photon cavity that draws much attention in recent experiments and notice the vibronic coupling predominately accounted for by the polarons. The most significant terms may remain, allowing the approximation  $g\sigma_i^\dagger D_l^\dagger \approx gD_l^\dagger \approx g$  in Eq. (3). The higher-order corrections will be presented elsewhere. We obtain an analytical solution to the 2D polariton signal (2DPS)

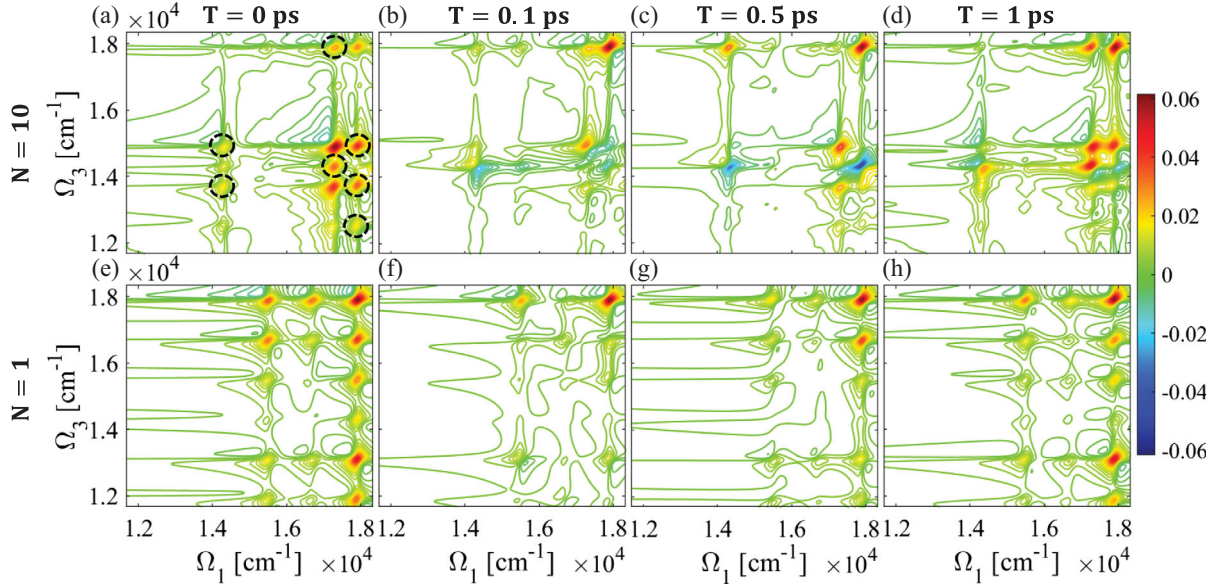


FIG. 2. 2D time- and frequency-resolved signal for molecular polaritons where (top)  $N = 10$  organic molecules and (bottom)  $N = 1$  organic molecule.  $T$  is varied, denoting the delay between the second and the third (probe) laser pulses. Horizontal and vertical axis are for absorption and emission frequencies, respectively.  $\lambda = 1$  and  $g\sqrt{N}/\omega_v = 1.5$ . Other parameters are the same as Fig. 1.

$$\begin{aligned}
 & S(\Omega_3, T, \Omega_1) \\
 &= ie^{i\phi} \sum_{i,l=1}^N \sum_{j,j'=1}^N \sum_{p=1}^{N+1} \sum_{\{m\}=0}^{\infty} S_{\{m\}}^{\lambda} \delta_{j'j}^{m_1} \delta_{il}^{m_2} \delta_{ji}^{m_3} \delta_{j'l}^{m_4} \\
 &\quad \times \delta_{ij}^{m_5} \delta_{i'j'}^{m_6} (-1)^{m_3+m_6} G_{il}(\Omega_3 + \xi_{m_2+m_5+m_6}) G_{lp}^*(T) G_{lj}(T) \\
 &\quad \times e^{i\xi_{m_3+m_4+m_5+m_6} T} \mathcal{G}_{p'j'}^*(-\Omega_1 - \xi_{m_1+m_4+m_6}) \quad (8)
 \end{aligned}$$

subsequently from Eq. (7), where  $S_{\{m\}}^{\lambda} = \prod_{s=1}^6 S_{m_s}^{\lambda}$  and  $\phi$  encodes a global phase from the four laser pulses. Details of the derivation of the signals via QLEs are given in Supplemental Material [57].

*Simulations.*—We have simulated the 2DPS to study molecular polariton dynamics from the analytical solutions. We set  $g\sqrt{N}/\omega_v = 1.5$  for strong coupling and a pulse duration of 10 fs.

The lower and upper rows in Fig. 2 illustrate the 2DPS, respectively, for  $N = 1$  and 10 molecules with fixed  $2g\sqrt{N}$ . For ten molecules in the cavity, the signal reveals the real-time population transfer and coherence dynamics between polaritons and EDSs. The EDSs, however, cannot be resolved with one molecule only. This is evident by the absence of the peaks at  $\Omega_{1,3} = \omega_D \pm n\omega_v$  ( $n = 0, 1, 2, \dots$ ) in the lower row. The 2DPS for  $N = 1$  can monitor the states at  $\omega_{UP} - \text{integer} \times \omega_v$  and their populations and coherence with the polariton states, as seen from the variation of the cross peaks with the time delay.

Figure 2(a) shows the 2D signal at  $T = 0$ . One observes the LP and UP states from the two diagonal peaks at  $\omega \pm g\sqrt{N}$ . The cross peaks may result from the coherence

and the polariton-polaron coupling, as there is no energy transport and dephasing at  $T = 0$ . The former is due to the broadband pump pulses (i.e.,  $3336 \text{ cm}^{-1}$  for a duration of 10 fs), whereas the latter is responsible for the change of phonon numbers associated with optical transitions. To have a closer look, we notice the states at  $\Omega_1 = 14300, 17300$ , and  $17900 \text{ cm}^{-1}$ . These agree with the absorbance in Fig. 1(c) (top). The cross peaks imposing  $\Omega_1 - \Omega_3 = \text{integer} \times \omega_v$  indicates the population of the EDSs which decouple from cavity photons and emit phonons, for instance, those at  $(\Omega_1 = 17300 \text{ cm}^{-1}, \Omega_3 = 14900 \text{ cm}^{-1})$  and  $(\Omega_1 = 17300 \text{ cm}^{-1}, \Omega_3 = 13700 \text{ cm}^{-1})$ . The EDSs erode molecular cooperativity and are highly degenerated, having the frequency  $\omega_D \pm n\omega_v$ ;  $n = 1, 2, \dots$ . The cross peaks with  $\Omega_1 - \Omega_3 \neq \text{integer} \times \omega_v$  as circled in Fig. 2(a) come from the superposition of excited states, e.g., the one at  $(\Omega_1 = 17900 \text{ cm}^{-1}, \Omega_3 = 14900 \text{ cm}^{-1})$  for  $\alpha|\omega_D - \omega_v\rangle + \beta|\omega_{UP}\rangle$ . The peaks at EDSs in  $S_{2D}(\Omega_3, 0, \Omega_1)$  manifest the vibronic coupling that may erode the collective motion of exciton polaritons, even at steady state [21].

When the delay  $T$  varies, Fig. 2(b) shows the fast decay of the coherence. This can be seen prominently from the decreasing intensities of the cross peaks with  $\Omega_1 - \Omega_3 \neq \text{integer} \times \omega_v$ , compared to Fig. 2(a). From Fig. 2(b), nevertheless, one can observe the cross peak at  $(\Omega_1 = 17900 \text{ cm}^{-1}, \Omega_3 = 14900 \text{ cm}^{-1})$  whose intensity increases after a rapid decay with the delay  $T$ . This describes the downhill energy transfer from UP to the EDS  $\omega = \omega_D - \omega_v = 14900 \text{ cm}^{-1}$ , following a fast dephasing. An energy transfer to LP can also be seen from the growth of

the cross peak at ( $\Omega_1 = 17\,900\text{ cm}^{-1}$ ,  $\Omega_3 = 14\,300\text{ cm}^{-1}$ ). Similarly, the energy transfer pathway from the EDS  $\omega = \omega_D + \omega_v = 17\,300\text{ cm}^{-1}$  to the LP can be observed within about 300 fs. Observing the weak intensity along with a slow growth at the cross peaks ( $\Omega_1 = 17\,900\text{ cm}^{-1}$ ,  $\Omega_3 = \omega_D - n\omega_v$ ) in Figs. 2(b) and 2(c), the system is slightly localized from the UP state within  $\sim 500$  fs because of the weak populations of EDSs. During a longer timescale  $T > 500$  fs, Figs. 2(c) and 2(d) evidence that the energy flowing from UP and state  $\omega = \omega_D + \omega_v = 17\,300\text{ cm}^{-1}$  to the EDS  $\omega = \omega_D - \omega_v = 14\,900\text{ cm}^{-1}$  dominates. A strong localization of the system, thus, emerges. This can be neatly understood from the Fermi's golden rule  $\Gamma_{i \rightarrow f} = 2\pi |\langle f|V|i\rangle|^2 N_i D_f$  by noting a larger number of EDSs than polaritons. From the slice  $\Omega_1 = \omega_D + \omega_v = 17\,300\text{ cm}^{-1}$ , the system tends to be alternatively delocalized within a longer timescale  $T > 500$  fs; Figs. 2(c) and 2(d) show the strong peak intensity at LP that indicates the population transferred considerably.

Moreover, most of the cross peaks in Fig. 2 appear below the diagonal, as a result of the low temperature, i.e.,  $\omega_v/T_b \gg 1$ . During the first 250 fs, the fast decay of the cross peak at ( $\Omega_1 = 14\,300\text{ cm}^{-1}$ ,  $\Omega_3 = 14\,900\text{ cm}^{-1}$ ) monitors the decay of superposition  $\alpha|\omega_{LP}\rangle + \beta|\omega_D - \omega_v\rangle$ . The population transfer from the LP to the EDS  $\omega = \omega_D - \omega_v = 14\,900\text{ cm}^{-1}$  emerges for longer delay, as indicated from the cross peak at ( $\Omega_1 = 14\,300\text{ cm}^{-1}$ ,  $\Omega_3 = 14\,900\text{ cm}^{-1}$ ) that increases within about 750 fs. Besides, the cross peak at ( $\Omega_1 = 14\,300\text{ cm}^{-1}$ ,  $\Omega_3 = 17\,900\text{ cm}^{-1}$ ) shows up weakly within about 500 fs, as depicted in Fig. 2(c). A small portion of energy transferred from LP to UP is, thus, indicated. As such, one may infer a cascading population transfer between two polariton states within a short timescale. In longer timescales, this is expected to deplete.

*Relation to the pump-probe signal.*—The pump-probe signal can be readily obtained by letting  $T_1 = T_2$  in Eq. (7) and accounting for the nonrephasing component. The signal reads  $S_{pp}(\omega, T) = \text{Im}[E_3^*(\omega)P(\omega)]$  so that

$$S_{pp}(\omega, T) = \sum_{i,l=1}^N \sum_{j,j'=1}^N \sum_{\{m\}=0}^{\infty} S_{\{m\}}^\lambda \delta_{il}^{m_1} (\delta_{jl} - \delta_{jl})^{m_2} (\delta_{ij} - \delta_{ij'})^{m_3} \times \text{Re}[\mathcal{G}_{il}(\omega + \xi_{m_1+m_3}) G_{ij'}^*(T) G_{ij}(T) e^{i\xi_{m_2+m_3}T}] \quad (9)$$

under the impulsive approximation. The ultrashort pulses smear out the mode selectivity in the absorption, whereas the time grating makes the emission spectrally resolved. Similar as the 2DPS, the LP and UP modes separated by  $2g\sqrt{N}$  as well as the EDSs at  $\omega = \omega_D - m\omega_v$  can be resolved in  $S_{pp}(\omega, T)$ . As varying the time delay, the spectral-line intensity  $S_{pp}(\omega_{UP/LP}, T)$  shows a phase difference from the  $S_{pp}(\omega_D - m\omega_v, T)$ , associated with different

damping rates that are responsible for the incoherent channels of relaxations [61].

*Summary and outlook.*—The microscopic theory of multidimensional spectroscopy for the molecular polaritons was developed, using the quantum Langevin equation capable of polariton-polaron interactions. Rich information about the fast-evolving dynamics of polaritons and dark states and their couplings can be readily visualized in the 2DPS. Our Letter manifests the ultrafast polariton-polaron interaction in molecules, resolving the EDSs against the polariton dynamics. This falls into a different category from the cavity QED for atoms, where no relaxation between superradiant and subradiant states can be observed [62–64]. Our model used a simplified description for aggregated molecules, i.e., a group of two-level systems coupled to intramolecular vibrations undergoing the Brownian oscillation. To account for photochemistry including geometric phases, extensive efforts will be devoted to the anharmonicity and multilevel systems, so as to generalize present work to approach realistic systems with complex potential energy. This may, however, need heavier loads of numerical methods. Our Letter would be insightful for the study of polariton-afforded molecular relaxation and cavity-coupled heterostructures.

*Remarks.*—It is worth noting that Eq. (7) provides a general form of the signal to involve the pulse shape effects beyond the impulsive approximation used in Eqs. (8) and (9). This yields a certain window of selective access of molecular excited states, which is indeed a subtle issue in pump-probe scheme rather than the 2D case. A complete understanding of the pump-probe spectroscopy for molecular polaritons, therefore, needs a delicate treatment on top of Eq. (7), so as to incorporate the pulse shape effects. These will be presented elsewhere.

Z. Z. gratefully acknowledges the support of the Early Career Scheme from Hong Kong Research Grants Council (No. 21302721), the National Science Foundation of China (No. 12104380), and the National Science Foundation of China/RGC Collaborative Research Scheme (No. CRS-CUHK401/22). D. L. gratefully acknowledges the support of the National Science Foundation of China, the Excellent Young Scientist Fund (No. 62022001). S. M. thanks the support of the National Science Foundation (No. CHE-1953045) and of the U.S. Department of Energy, Office of Science, Basic Energy Sciences, under Grant No. DE-SC0022134.

\*zzhan26@cityu.edu.hk

†smukamel@uci.edu

- [1] A. Thomas, J. George, A. Shalabney, M. Dryzhakov, S. J. Varma *et al.*, *Angew. Chem., Int. Ed.* **55**, 11462 (2016).
- [2] J. Hutchison, T. Schwartz, C. Genet, E. Devaux, and T. W. Ebbesen, *Angew. Chem.* **124**, 1624 (2012).
- [3] A. D. Dunkelberger, B. T. Spann, K. P. Fears, B. S. Simpkins, and J. C. Owrutsky, *Nat. Commun.* **7**, 13504 (2016).

- [4] X. Li, A. Mandal, and P. Huo, *Nat. Commun.* **12**, 1315 (2021).
- [5] F. Herrera and F. C. Spano, *Phys. Rev. Lett.* **116**, 238301 (2016).
- [6] L. Martinez-Martinez, R. Ribeiro, J. Campos-Gonzalez-Angulo, and J. Yuen-Zhou, *ACS Photonics* **5**, 167 (2018).
- [7] D. M. Coles, N. Somaschi, P. Michetti, C. Clark, P. G. Lagoudakis, P. G. Savvidis, and D. G. Lidzey, *Nat. Mater.* **13**, 712 (2014).
- [8] M. Kowalewski, K. Bennett, and S. Mukamel, *J. Phys. Chem. Lett.* **7**, 2050 (2016).
- [9] J. Galego, F. J. Garcia-Vidal, and J. Feist, *Nat. Commun.* **7**, 13841 (2016).
- [10] S. Aberra Guebrou, C. Symonds, E. Homeyer, J. C. Plenet, Yu. N. Gartstein, V. M. Agranovich, and J. Bellessa, *Phys. Rev. Lett.* **108**, 066401 (2012).
- [11] F. C. Spano, *J. Chem. Phys.* **142**, 184707 (2015).
- [12] A. Shalabney, J. George, J. Hutchison, G. Pupillo, C. Genet, and T. W. Ebbesen, *Nat. Commun.* **6**, 5981 (2015).
- [13] J. Flick, M. Ruggenthaler, H. Appel, and A. Rubio, *Proc. Natl. Acad. Sci. U.S.A.* **114**, 3026 (2017).
- [14] S. Mukamel, *Principles of Nonlinear Optical Spectroscopy* (Oxford University Press, Oxford, 1999).
- [15] D. Wang, H. Kelkar, D. Martin-Cano, D. Rattenbacher, A. Shkarin, T. Utikal, S. Götzinger, and V. Sandoghdar, *Nat. Phys.* **15**, 483 (2019).
- [16] E. Hulkko, S. Pikker, V. Tiainen, R. H. Tichauer, G. Groenhof, and J. J. Toppari, *J. Chem. Phys.* **154**, 154303 (2021).
- [17] K. Georgiou, R. Jayaprakash, A. Askitopoulos, D. M. Coles, P. G. Lagoudakis, and D. G. Lidzey, *ACS Photonics* **5**, 4343 (2018).
- [18] M. Tavis and F. W. Cummings, *Phys. Rev.* **170**, 379 (1968).
- [19] M. Gross and S. Haroche, *Phys. Rep.* **93**, 301 (1982).
- [20] F. C. Spano, J. R. Kuklinski, and S. Mukamel, *Phys. Rev. Lett.* **65**, 211 (1990).
- [21] Z. D. Zhang, K. Wang, Z. Yi, M. S. Zubairy, M. O. Scully, and S. Mukamel, *J. Phys. Chem. Lett.* **10**, 4448 (2019).
- [22] F. J. Garcia-Vidal, J. Feist, and J. del Pino, *New J. Phys.* **17**, 053040 (2015).
- [23] F. Herrera and F. C. Spano, *Phys. Rev. Lett.* **118**, 223601 (2017).
- [24] M. Reitz, C. Sommer, and C. Genes, *Phys. Rev. Lett.* **122**, 203602 (2019).
- [25] F. C. Spano and C. Silva, *Annu. Rev. Phys. Chem.* **65**, 477 (2014).
- [26] O. Vendrell, *Phys. Rev. Lett.* **121**, 253001 (2018).
- [27] B. Xiang, R. F. Ribeiro, A. D. Dunkelberger, J. Wang, Y. Li, B. S. Simpkins, J. C. Owrutsky, J. Yuen-Zhou, and W. Xiong, *Proc. Natl. Acad. Sci. U.S.A.* **115**, 4845 (2018).
- [28] K. E. Dorfman and S. Mukamel, *Proc. Natl. Acad. Sci. U.S.A.* **115**, 1451 (2018).
- [29] Z. D. Zhang, P. Saurabh, K. E. Dorfman, A. Debnath, and S. Mukamel, *J. Chem. Phys.* **148**, 074302 (2018).
- [30] Z. D. Zhang, T. Peng, X. Y. Nie, G. S. Agarwal, and M. O. Scully, *Light: Sci. Appl.* **11**, 274 (2022).
- [31] T. W. Ebbesen, *Acc. Chem. Res.* **49**, 2403 (2016).
- [32] F. Caruso, S. K. Saikin, E. Solano, S. F. Huelga, A. Aspuru-Guzik, and M. B. Plenio, *Phys. Rev. B* **85**, 125424 (2012).
- [33] F. Herrera, B. Peropadre, L. A. Pachon, S. K. Saikin, and A. Aspuru-Guzik, *J. Phys. Chem. Lett.* **5**, 3708 (2014).
- [34] B. Xiang, R. F. Ribeiro, Y. Li, A. D. Dunkelberger, B. B. Simpkins, J. Yuen-Zhou, and W. Xiong, *Sci. Adv.* **5**, eaax5196 (2019).
- [35] B. Xiang, J. Wang, Z. Yang, and W. Xiong, *Sci. Adv.* **7**, eabf6397 (2021).
- [36] Z. D. Zhang and S. Mukamel, *Chem. Phys. Lett.* **683**, 653 (2017).
- [37] M. A. Zeb, P. G. Kirton, and J. Keeling, *ACS Photonics* **5**, 249 (2018).
- [38] J. Galego, F. J. Garcia-Vidal, and J. Feist, *Phys. Rev. X* **5**, 041022 (2015).
- [39] A. Csehi, Á. Vibók, G. J. Halász, and M. Kowalewski, *Phys. Rev. A* **100**, 053421 (2019).
- [40] M. Du and J. Yuen-Zhou, *Phys. Rev. Lett.* **128**, 096001 (2022).
- [41] J. Gu, V. Walther, L. Waldecker, D. Rhodes, A. Raja, J. C. Hone, T. F. Heinz, S. Kéna-Cohen, T. Pohl, and V. M. Menon, *Nat. Commun.* **12**, 2269 (2021).
- [42] S. Mukamel, *J. Chem. Phys.* **145**, 041102 (2016).
- [43] J.-H. Zhong *et al.*, *Nat. Commun.* **11**, 1464 (2020).
- [44] V. M. Axt and S. Mukamel, *Rev. Mod. Phys.* **70**, 145 (1998).
- [45] L. Lacombe, N. M. Hoffmann, and N. T. Maitra, *Phys. Rev. Lett.* **123**, 083201 (2019).
- [46] M. Kowalewski, K. Bennett, and S. Mukamel, *J. Chem. Phys.* **144**, 054309 (2016).
- [47] J. Flick, H. Appel, M. Ruggenthaler, and A. Rubio, *J. Chem. Theory Comput.* **13**, 1616 (2017).
- [48] M. Gudem and M. Kowalewski, *J. Phys. Chem. A* **125**, 1142 (2021).
- [49] H.-P. Breuer and F. Petruccione, *The Theory of Open Quantum Systems* (Oxford University Press, Oxford, 2002).
- [50] N. T. Phuc, *J. Chem. Phys.* **155**, 014308 (2021).
- [51] F. Herrera and F. C. Spano, *Phys. Rev. A* **95**, 053867 (2017).
- [52] R. Saez-Blazquez, J. Feist, E. Romero, A. I. Fernandez-Domínguez, and F. J. García-Vidal, *J. Phys. Chem. Lett.* **10**, 4252 (2019).
- [53] Y. Tanimura, *J. Phys. Soc. Jpn.* **75**, 082001 (2006).
- [54] We have adopted the Condon approximation that  $\mu_{eg}$  is independent of the nuclear coordinates [14,55].
- [55] Y. J. Yan and S. Mukamel, *J. Chem. Phys.* **94**, 179 (1991).
- [56] C. A. Guarín, J. P. Villabona-Monsalve, R. López-Arteaga, and J. Peon, *J. Phys. Chem. B* **117**, 7352 (2013).
- [57] See Supplemental Material at <http://link.aps.org/supplemental/10.1103/PhysRevLett.130.103001> for a detailed description of the 2D coherent signal with the quantum Langevin equation.
- [58] J. Franck, *Trans. Faraday Soc.* **21**, 536 (1925).
- [59] Y.-C. Cheng and G. R. Fleming, *Annu. Rev. Phys. Chem.* **60**, 241 (2009).
- [60] J. Cao and R. J. Silbey, *J. Phys. Chem. A* **113**, 13825 (2009).
- [61] The low spectral resolution with the absorption process, however, makes the pump-probe signal not capable of unveiling advanced information about the polariton dynamics and dark states, e.g., relaxation pathways and timescales. More details are given in Supplemental Material [57].
- [62] D. Pavolini, A. Crubellier, P. Pillet, L. Cabaret, and S. Liberman, *Phys. Rev. Lett.* **54**, 1917 (1985).
- [63] W. Guerin, M. O. Araujo, and R. Kaiser, *Phys. Rev. Lett.* **116**, 083601 (2016).
- [64] R. E. Evans *et al.*, *Science* **362**, 662 (2018).